

Detecting changes in Precipitation Extremes Using Global Circulation Models in the Ogun – Osun River Basin, South West Nigeria

Okogbue, E.C.^{1*}; Balogun, I.A.^{1,3}; Akinbobola, A.¹; Adeyeri, O.^{1,4}; Oluleye, A.¹; Ajayi, V.O.¹; Akinluyi, F.O.²; Akinwumiju, A.S.², Ige, S.O.⁵ and Raji, I. A.¹

1Department of Meteorology & Climate Science, Federal University of Technology, Akure, Nigeria

2Department of Remote Sensing & GIS, Federal University of Technology, Akure, Nigeria

3Doctoral Research Programme in West African Science, West African School on Climate and Adapted Land Use, Akure, Nigeria

4Institute for Meteorology and Climate Research Atmospheric Environmental Research, Karlsruhe Institute of Technology, Campus Alpine, Germany

5Nigerian Meteorological Agency, Lagos, Nigeria

*Corresponding Author: Okogbue, E. C. (Emails: ecokogbue@futa.edu.ng; emokogbue@gmail.com)

Abstract

The study evaluates the projected changes in precipitation extremes over the Ogun-Osun River basin. The study was carried out using the ensemble mean of selected CORDEX models. Precipitation extremes were detected using indices such as the Annual total wet-day (prcptot), consecutive wet days (CWD), consecutive dry days (CDD), Total annual RR from very heavy rain days (R99p), Total annual RR from heavy rain days (R95p), Number of heavy rain days (R10mm). These indices were computed for both the historical (1979 - 2005) and the projection periods (2030–2070) under the RCP4.5 and RCP8.5 scenarios. The results show an increase in the extremes for the projection period with more severity under the RCP8.5 scenario. It can be deduced from the analysis that the projection periods are expected to have increased frequency of flash flood and drought occurrence.

Introduction

In recent decades, there has been an increase in the frequency, intensity and extent of the impact of natural disasters on the environment which is a concern to many nations. In many

West African countries, there has been an increase in the frequency of flood events, which has been attributed to climate change, leading to the loss of human lives and properties (Seydou et al, 2023). For the California drought (2012-2014), Mao *et al.* (2015) reported that warmer temperatures greatly influence river discharge while Williams *et al.* (2015) stated that increasing temperature escalates drought conditions. Over the Colorado Basin, Vano *et al.* (2012) reported that warmer temperatures reduce the discharge from Colorado River. Conversely, Reynolds *et al.* (2015) reported that the drying frequencies of intermittent streams in that basin are caused by changes occurring in both temperature and precipitation.

At a regional scale, significant correlations have been observed between monthly mean temperature and precipitation in Europe and North America (Madden & Williams 1978). Rusticucci & Penalba (2000) established a positive correlation between warm summers and low precipitation in the north-eastern and

central-western parts of Argentina, Paraguay and southern Chile. They further reported a significant and positive correlation between precipitation and temperature in the coastal parts of Chile especially between May and September as a result of high sea surface temperature which favours convection. Nicholls (2004) reported increased potential evaporation as a result of higher mean values of maximum and minimum temperatures, thereby enhancing the severity of the 2002 Australian drought.

Over Ghana, Neumann *et al.* (2007) showed an increase of almost 0.3 °C/decade in the near-surface temperature during both wet and dry seasons in the past three decades. Likewise, Adeyeri *et al.* (2019a) noted a significant positive trend in annual total rainfall, number of consecutive dry days, warm spell duration, warm day-, and warm night frequencies over the Komadougou-Yobe Basin (KYB). They also projected more frequent extreme precipitation and temperature events in the future. Adeyeri *et al.* (2019b) observed an increasing trend in annual precipitation and river discharge over the KYB between 1971 and 2013. Abiodun *et al.* (2017) examined the impacts of climate change on characteristics of extreme precipitation events over four African coastal cities under two future emission scenarios (RCP4.5 and RCP8.5). They reported an increase in dry spells and a decrease in wet days over the four cities in the future (2031–2065).

Previous studies have shown difficulty of GCMs in accounting for the impact of the complex topography on synoptic-scale features and mesoscale atmospheric systems that favour extreme precipitation due to the coarse spatial resolution of the GCM simulations and projections (Mason and Joubert, 1997; Shongwe *et al.* 2009). To bridge this gap

between large scale and local scale, several studies have downscaled GCM projections with RCMs (e.g. Engelbrecht *et al.*, 2009; Klutse *et al.*, 2014; Dieng *et al.*, 2017, Adeyeri *et al.*, 2020a).

Regardless of this development, only a few studies have utilised the CORDEX dataset in providing multi-RCM future projections for climate extremes in Africa e.g. on precipitation extremes over Southern Africa (Pinto *et al.*, 2016).

Furthermore, the use of extreme indices for climate extremes analysis is based on the exceeding threshold or probability of occurrence of a given variable. Results from various studies in Africa (e.g. Ly *et al.*, 2013; Abatan *et al.*, 2017a; Adeyeri *et al.*, 2019b) showed no uniform pattern in the trend of annual precipitation as it depends on the locality. Overall, the different patterns of the above results encourage continuing analysing the climate extremes for several spatial scales (e.g. the regional-, local-, or watershed scale). Okogbue *et al.* (2021) analysed the drainage morphometry and land use/land cover Dynamics of the of the ogun-osun River basin and observed from the stream frequency, infiltration number, drainage density analysis, the potential for surface runoff, flood and erosion differ across the basin.

To proffer solutions to the problems associated with water resources management within the Osun-Ogun River Basin (ORB), there is need to understand the relationship between these variables at the basin's scale since the spatio-temporal behaviour of precipitation depend on the regional and local forcings. Therefore, this study seeks to improve the understanding of the relationships in the observed trends of precipitation over the ORB between 1979 and 2019. Our approaches include trend analyses at both temporal and spatial scales, correlation

and wavelet analyses among the variables. Furthermore, the trends in extreme rainfall indices in the ORB are examined using the observations (1979–2017), regional climate model simulations for the past (1979–2005) and the future projection (2030–2070).

2 Data and Methodology

The Ogun-Osun River Basin, situated in southwestern Nigeria, is a crucial geographical and socioeconomic region spanning five states. It is characterized by a network of rivers, primarily the Ogun and Osun rivers. The tropical climate, with distinct rainy and dry seasons, influences water availability and the region's ecosystems, affecting the distribution of plant and animal species (Longe et al, 2010).

The analyses utilized ERA 5 daily maximum temperature, minimum temperature and rainfall from 1979 to 2019 archived by the European Centre for Medium-Range Weather Forecasts with a resolution of 0.25° . Although, the

In this regard, six precipitation indices (Table 1), namely number of heavy rain days when rainfall is at least 10mm (R10mm), consecutive dry days (cdd), consecutive wet days (cwd),

uncertainties associated with climate change impact assessment on extreme indices cannot be under-emphasised. This includes GCM and RCM configurations and RCP scenarios. However, in this study, the uncertainty range is minimized by analysing the model ensemble mean of CORDEX data comprising of eight GCMs (Table 2) dynamically downscaled by one RCM, i.e. the RCA4 (Swedish Meteorological and Hydrological Institute-Rosby Centre Atmosphere model version 4) which has a resolution of $0.44^{\circ} \times 0.44^{\circ}$. This is used for the future projection (2030–2070) under two representative concentration pathways (RCP 4.5 and RCP 8.5) while the simulated historical was between 1979 and 2005. This RCM is chosen due to its performance over West Africa and particularly its ability to adequately reproduce West Africa rainfall regimes (Akinsanola et al., 2017; Yira et al., 2017; Adeyeri et al., 2019a).

amount of rainfall from very wet days (r95p), amount of rainfall from extremely wet days (r99p), and annual total rainfall (prcptot) have been analysed for these periods.

Table 1: List of GCMs used as boundary conditions for the Rossby Centre Regional Atmospheric (RCA) model

S/N	Modelling Centre	GCM
1	Canadian Centre for Climate Modelling and Analysis	CanESM2
2	Centre National de Recherches Météorologiques/Centre Européen de Recherche et Formation Avancée en Calcul Scientifique	CNRM-CM5
3	EC-EARTH consortium	EC-EARTH
4	NOAA Geophysical Fluid Dynamics Laboratory	GFDL-ESM2M
5	Met Office Hadley Centre	HadGEM2-ES
6	Atmosphere and Ocean Research Institute (The University of Tokyo), National Institute for Environmental Studies and Japan Agency for Marine-Earth Science and Technology	MIROC5
7	Max Planck Institute for Meteorology	MPI-ESM-LR
8	Norwegian Climate Centre	NorESM1-M

Table 2: Climate indices used below

Short name	Long name	Definition	Description	Unit
R10mm	Number of heavy rain days	Number of days when $RR \geq 10\text{mm}$	Days when rainfall is at least 10mm	days/decade
CWD	Consecutive Wet Days	Maximum annual number of consecutive wet days (when $RR \geq 1\text{mm}$)	The longest wet spell	days/decade
R95p	Total annual RR from heavy rain days	Annual sum of daily PR $> 95\text{th}$ Percentile	Amount of rainfall from very wet days	mm/decade
R99p	Total annual RR from very heavy rain days	Annual sum of daily PR $> 99\text{th}$ Percentile	Amount of rainfall from extremely wet days	mm/decade
PRCPTOT	Annual total wet-day RR	Sum of daily PR ≥ 1.0 mm	Total wet-day rainfall	mm/decade
CDD	Consecutive Dry Days	Maximum annual number of consecutive dry days (when $RR < 1\text{mm}$)	The longest dry spell	days/decade

Bias correction (BC) minimizes discrepancies between observed and simulated climate variables. The GCM models ensemble was bias corrected as described in Amengual et al., 2012 and Adeyeri et al., 2019a. The modified Mann-Kendall (mMK) trend test as described in Adeyeri et al. (2017) was used to analyze the trend of the climatic variables and the magnitude of the trend is estimated using the Theil and Sen's slope estimator.

3 Results

3.1 Climatology of the Basin

Figure 1 shows the climatological mean for the daily precipitation

values. The daily climatological mean over the study area generally ranges between 1 and 6 mm/day over 40 years. The southeastern part of the basin records higher magnitude between 4 to 6 mm/day while the northern region averages 1-3 mm/day. The spatial distribution of the daily mean minimum temperature climatology shows the northern region having daily average values of 21oC to 23oC and values greater than 25oC in the southern region while the mean maximum daily temperature a northern maximum with value greater than 30oC and 28oC in the Southern part

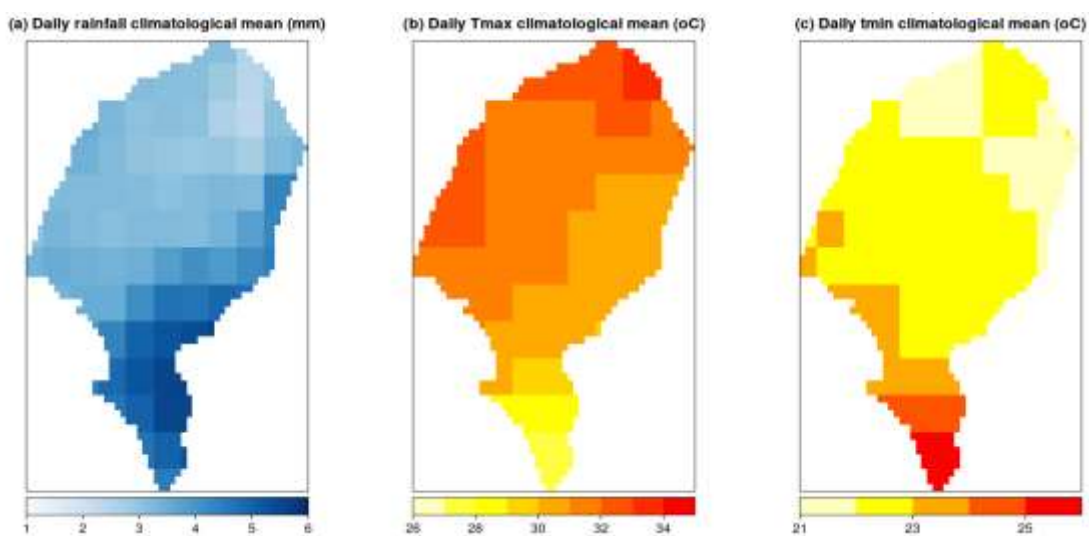


Figure 1: Spatial climatological mean for daily Rainfall (mm)

The trend analysis shows an increasing trend of 0.02 °C/year in both Tmax and Tmin (Figure 2) with an average increase of 0.5°C is observed in both maximum and

minimum temperature between 1980 and 2020. Conversely, a decreasing trend of 2.65 mm/year in rainfall across the basin (Figure 3).

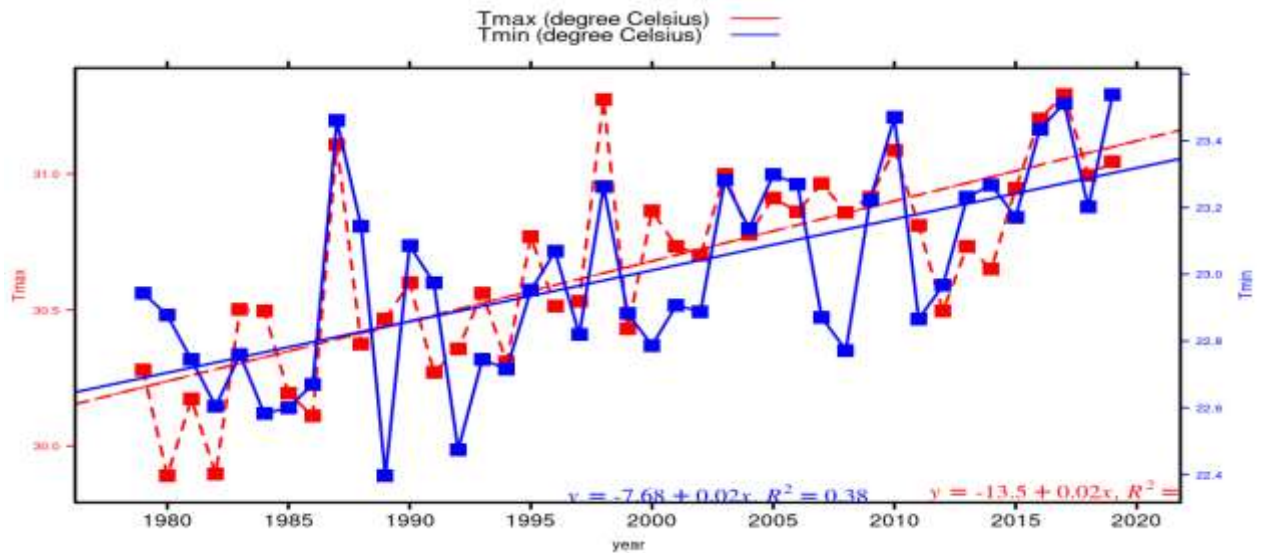


Figure 2: Annual trend of Areal Tmax and Tmin

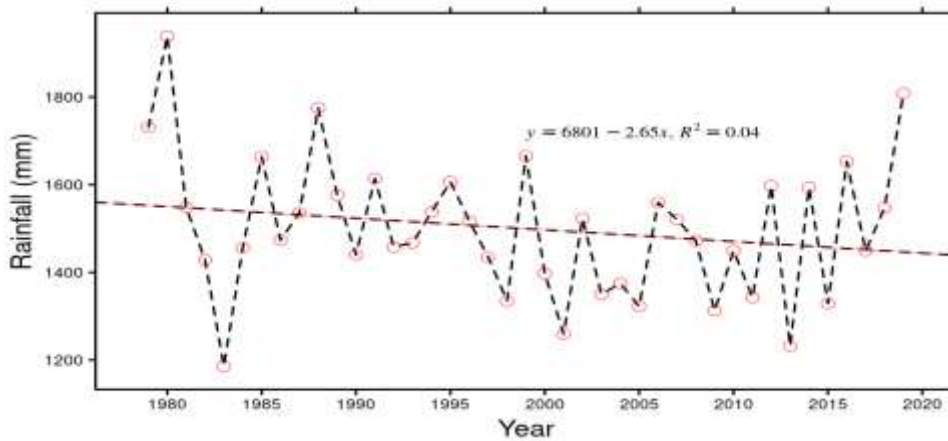


Figure 3: Annual trend of Areal Rainfall

3.2 Climate Indices

This section explains the results of the different climate indices chosen for this study.

3.2.1 Historical Period

Consecutive Dry Days (CDD) and Consecutive Wet Days (CWD)

Figure 4 shows the climatological mean and trend of the consecutive dry days (CDD) and consecutive wet days (CWD) in the basin. The climatological mean for the CDD ranges from 15 to 115 days, between 1979 and 2019, while lowest values of between 15 and 35 days are located at the southern part of the basin. The northern edge of the basin has the highest values. Conversely, the lowest values of the CWD is located at the northern part of the basin. Furthermore, the trend of the CDD increases between 0 to 10 days/decade. However, the most increase is at the northern part of the basin with 10

days/decade while the southern part increases between 0 to 2 days/decade. The CWD trend on the other hand ranges between -10 to 1 day/decade. The most decrease is located at the southern part of the basin. Also, the trends in CDD and CWD are significant at 95% confidence level in most parts of the basin (4 e and f). The decreasing trend observed for the CWD implies reduced frequency of flood occurrence during the historical period in the region. Prolonged dry spells could result due to observed increasing trend of CDD in reduced river flow and lower groundwater levels, causing water scarcity for both humans and wildlife. This has also led to drought conditions, which have negatively impacted agriculture and food security (Eltahir and Gong, 2002).

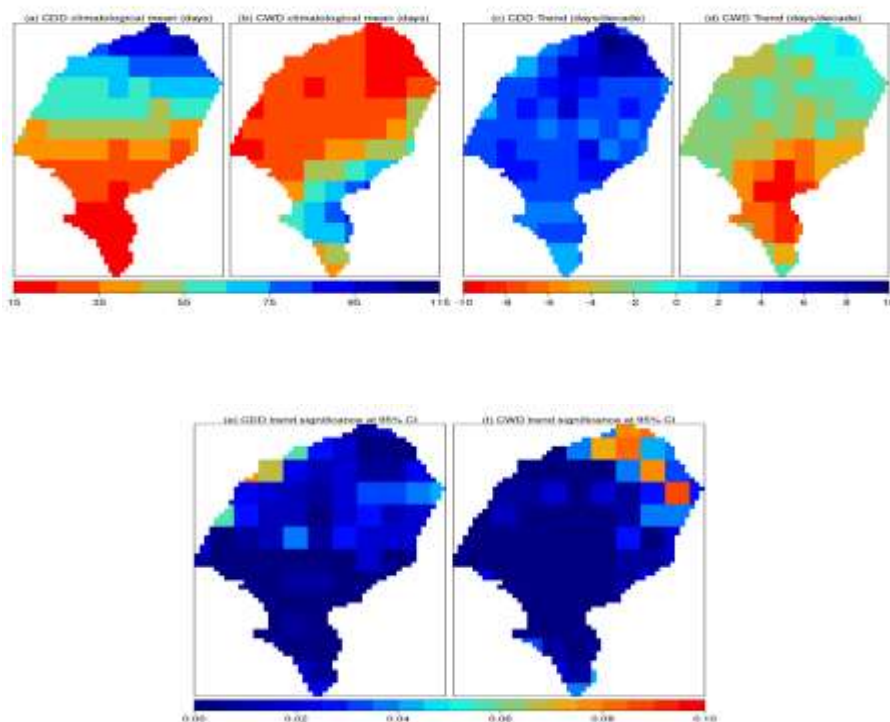


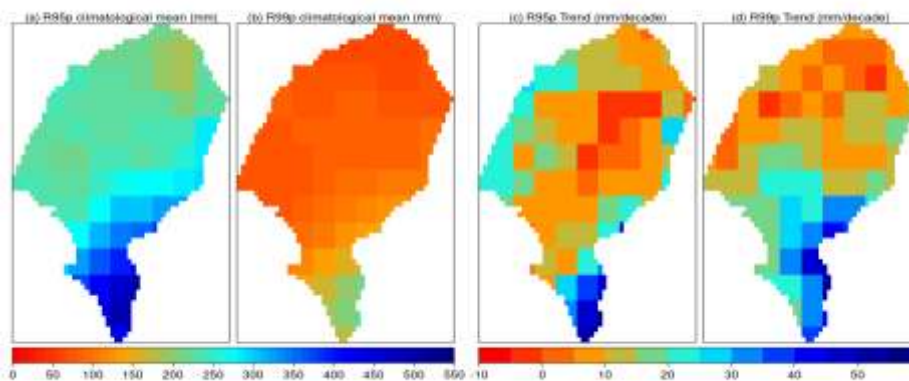
Figure 4: Climatological mean (a and b), trend (c and d) and trend significance (e and f) in CDD and CWD in the basin

Total annual rainfall from heavy rain days (R95p) and Total annual rainfall from very heavy rain days (R99p)

Figure 5 shows the climatological mean and trend of the total annual rainfall from heavy rain days (R95p) and total annual rainfall from very heavy rain days (R99p) in the basin.

The climatological mean for the R95p ranges from 200 to 550 mm between 1979 and 2019 while lowest values of between 200 and 250 mm are located at the northern part of the basin. Similarly, the lowest values of the R99p is located at the northern

part of the basin. Furthermore, the trend of the R95p increases generally in the basin except for some little parts in the middle of the basin (-10 mm/decade). The generally increasing trend is between 50 to 60 mm/decade. Similarly, the R99p trend increases between 0 and 60 mm/decade in most parts of the basin. Although there is a similarity in the quantity of R95p and R99p, however, the spatial distribution is different. Also, there is a mixture of significant and non-significant trends in R95p in the basin. However, the R99p trends are significant at 95% confidence level in most parts of the basin (5 e and f). The increasing trend of the R95p and R99p suggests that the area increased rainfall from heavy rain days can lead to increased flooding in the Ogun-Osun River Basin, with negative impacts on infrastructure, agriculture, and human communities



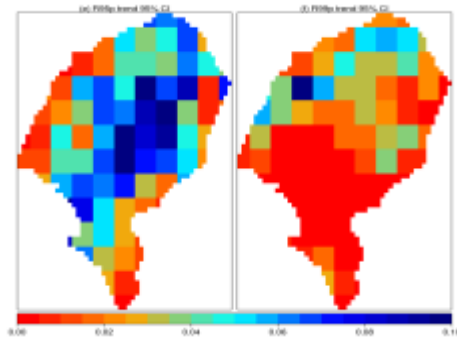


Figure 5: Climatological mean (a and b), trend (c and d) and trend significance (e and f) in R95p and R99p in the basin

Number of Heavy Rain Days (r10mm) and Total Wet Day Rainfall (prcptot)

Figure 6 shows the climatological mean and trend of the number of heavy rain days (r10mm) and total wet day rainfall (prcptot) in the basin.

The climatological mean for r10mm ranges from 20 to 70 days between 1979 and 2019 while the lowest values of between 20 and 35 mm are located at the northern part of the basin. The southern part of the basin has the highest values of between 50 to 70 mm. Similarly, the lowest values of the prcptot are located in the northern part of the basin. The values of prcptot increases from 800mm in the northern part to 2300mm in the southern part. Additionally, the trend of the r10mm increases generally in the

northern part of the basin with values between 0 and 1 mm/decade. However, the southern part is a predominantly negative trend. There is a generally decreasing trend of prcptot in the basin. However, the most northern part has an increasing trend of between 0 and 10 mm/decade.

Also, there is a predominant significant trend of r10mm in the southern part of the basin, however, prcptot trend is generally significant in most parts of the basin (6 e and f). This can be associated to the observed decrease in the CWD and observed general decrease in precipitation trend over the region. The increasing trend in the northern part suggests the area is prone to flash flood occurrences especially the Southern part of the region.

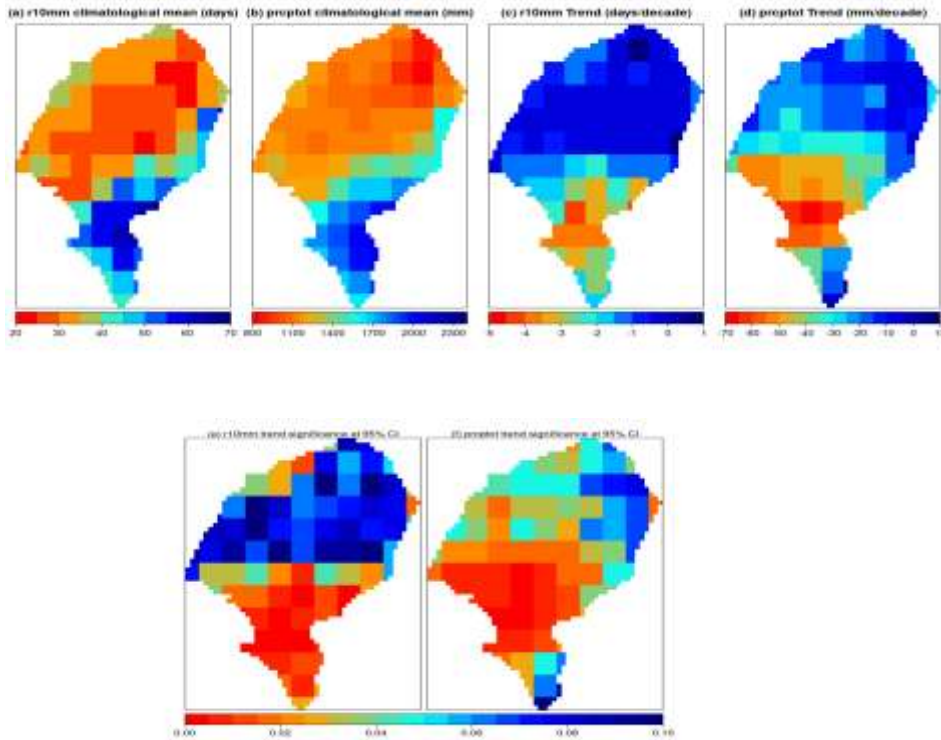


Figure 6: Climatological mean (a and b), trend (c and d) and trend significance (e and f) in r10mm and prcptot in the basin

3.2.2 Projection

Table 3 presents the validation results of the bias-corrected CORDEX and uncorrected CORDEX for the entire basin. The bias-corrected CORDEX performed better than the uncorrected CORDEX in reproducing the trends of the climate indices for the validation period between 1979 and 2005.

It is also able to capture the significant observed direction and magnitude in the indices. This provides the basis and confidence in using the bias correction method for future projections.

Table 2: Basin-scale trend of indices for the validation period from observed data, bias-corrected CORDEX and raw CORDEX between 1979 and 2005. Bold values represent a significant change in trend at 95% confidence interval

	Indices					
	Cdd	cwd	r95p	r99p	r10mm	prcptot
Validation period						

Slope	0.5	-0.6	-0.3	0.9	-0.4	-10.0
Bias-Corrected CORDEX						
Slope	0.7	-0.5	-0.5	1.2	-0.4	-8.8
RMSE	0.2	0.1	0.2	0.3	0	1.2
MSE	0.04	0.01	0.04	0.09	0	1.44
PBIAS	40	-16.7	66.7	33.3	0	-12
Uncorrected CORDEX						
Slope	1.3	-0.1	4.8	2.5	-0.2	-2
RMSE	0.8	0.5	5.1	1.6	0.2	8
MSE	0.64	0.25	26.01	2.56	0.04	64
PBIAS	160	-83.3	-1700	177.8	-50	-80

RMSE is the root mean square error, MSE is the mean square error and PBIAS is the percentage bias

Indices under RCP 4.5

Consecutive Dry Days (CDD) and Consecutive Wet Days (CWD)

Figure 7 shows the climatological mean and trend of the consecutive dry days (CDD) and consecutive wet days (CWD) in the basin. The climatological mean for the CDD ranges from 10 to 190 days between 2030 and 2070. This is an increment of between 5 and 75 days from the historical period. The lowest values of between 10 and 40 days are located at the southern part of the basin while the northern edge of the

basin has the highest values. Conversely, the lowest values of the CWD are located at the northern part of the basin. CWD for the entire basin ranges between 10 and 220 days. Furthermore, the trend of the CDD varies between 2 to 4 days/decade. The most increasing trends are found at the northern part of the basin with values between 0 and 4 days/decade. There is a generally increasing trend of CWD in the basin. The CWD trend values range from -22 to 4 days/decade. Both projected temperature increase and precipitation decrease under this scenario contributed greatly to the increase in the CDD index.

Also, the trends in CDD and CWD are most significant at 95% confidence level throughout the basin (e and f). Projected increasing trends in consecutive dry days (CDD) and consecutive wet days (CWD) can have significant impacts on flood occurrence in the river basin. Increasing CWD can lead to an increase in the

frequency and intensity of heavy precipitation events, which can result in increased runoff and flash flooding in the basin. The study also found that increasing CWD can cause rivers and streams to rise, leading to an increased risk of riverine flooding.

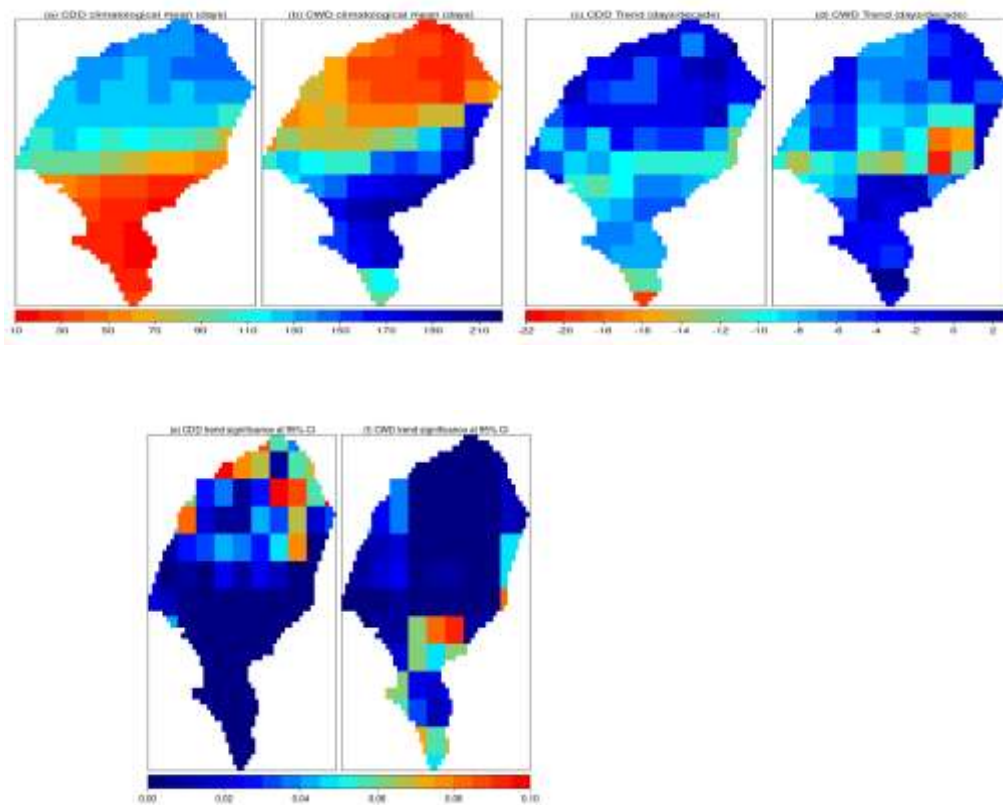


Figure 7: Climatological mean (a and b), trend (c and d) and trend significance (e and f) in CDD and CWD in the basin

Total annual rainfall from heavy rain days (R95p) and Total annual rainfall from very heavy rain days (R99p)

Figure 8 shows the climatological mean and trend of the total annual rainfall from heavy rain days (R95p) and total annual rainfall from very heavy rain days (R99p) in the basin.

The climatological mean for the R95p ranges from 300 to 800 mm between 2030 and 2070. This is an increment of between 100 to 250 mm from the historical period.

However, the lowest values are located in the northern part of the basin. The values for R99p range between 100 and 400 mm. Furthermore, the trend of the R95p decreases generally in the basin except for some little parts in the middle of the basin (0 - 10 mm/decade). The generally decreasing trend is between -100 to -10 mm/decade. Similarly, the R99p trend increases between 0 and 30 mm/decade in most parts of the basin. There is a reduction

in the magnitude of the trend compared to the historical period. Also, the R95p trend is most significant for the basin. A mixture of both significant and non-significant trend is observed in the basin (8 e and f). The climatological impact of the projected trend on the river basin is similar to the climatological impact that the CWD and CDD increasing trend are suggested to have (i.e increased risk of flooding occurrence).

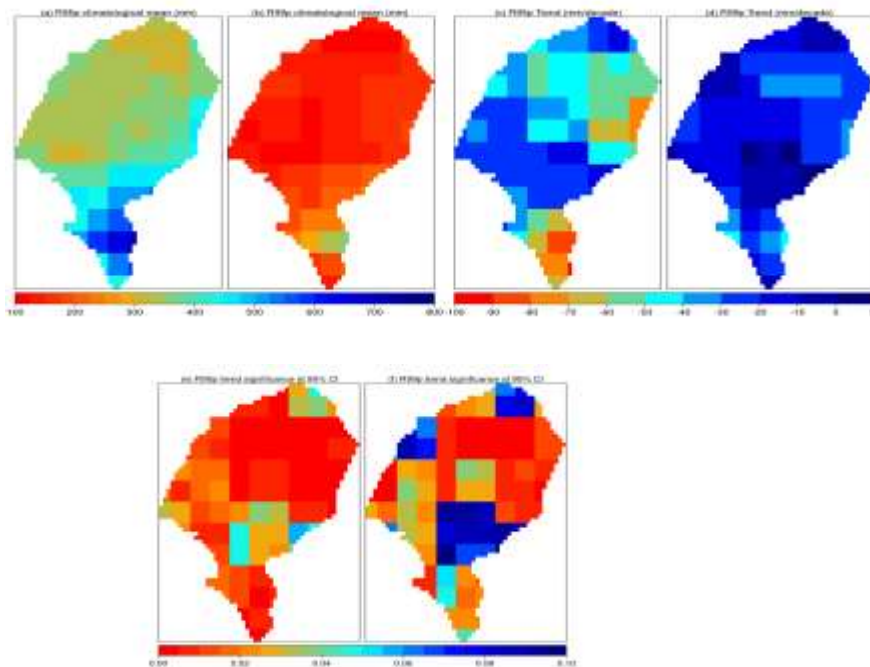


Figure 8: Climatological mean (a and b), trend (c and d) and trend significance (e and f) in R95p and R99p in the basin

Number of Heavy Rain Days (r10mm) and Total Wet Day Rainfall (prcptot)

Figure 9 shows the climatological mean and trend of the number of heavy rain days (r10mm) and total wet day rainfall (prcptot) in the basin.

The climatological mean for r10mm ranges from 20 to 90 days between 2030 and 2050. This is an increment of 20mm in the upper

bound from the historical period. The southern part of the basin has the highest values of between 50 to 90 mm. Similarly, the lowest values of the PRCPTOT are located at the northern part of the basin. The values of PRCPTOT increase from 900mm in the northern part to 2400mm in the southern part. This is also an increment of 100mm from the historical period. Additionally, the trend of the r10mm decreases generally in the entire basin with

values between -1 and -8 mm/decade. There is a generally decreasing trend of PRCPTOT in the basin with values between -120 and -20 mm/decade. Also, there is a predominant significant trend of r10mm in the basin, however, PRCPTOT trend is generally significant in the northern parts of the basin (9 e and f). This suggests that extreme precipitation events over the region will very likely become more intense and more frequent during the projection period

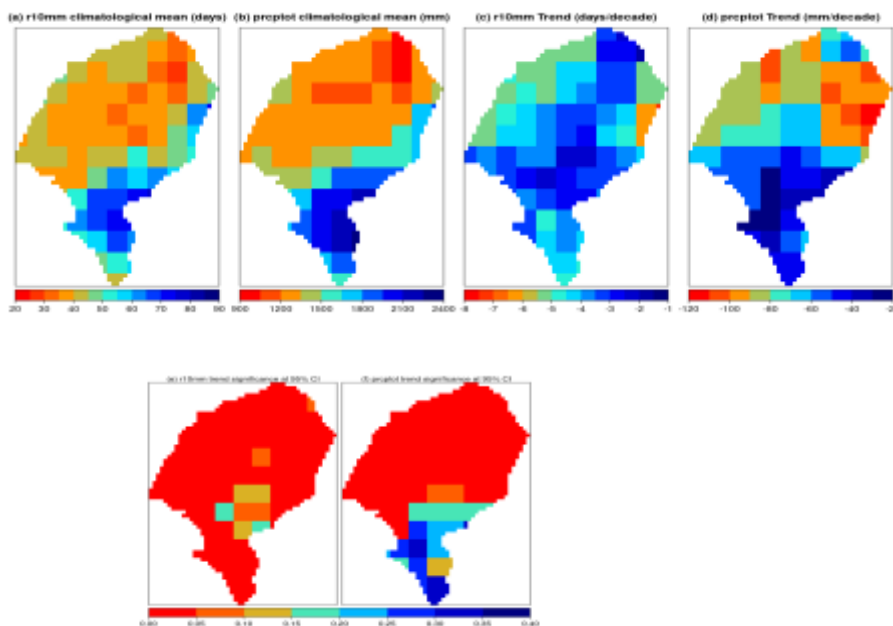


Figure 9: Climatological mean (a and b), trend (c and d) and trend significance (e and f) in r10mm and prectot in the basin

Indices under RCP 8.5

Consecutive Dry Days (CDD) and Consecutive Wet Days (CWD)

Figure 10 shows the climatological mean and trend of the consecutive dry days (CDD) and consecutive wet days (CWD) in the basin. The climatological mean for the

CDD ranges from 10 to 160 days between 2030 and 2070 under RCP 8.5. This is +45 and +60 days in the upper bounds from the historical period and future period under RCP 4.5 respectively. The lowest values of between 10 and 60 days are located at the southern part of the basin while the northern edge of the basin has the highest values. Contrariwise, the lowest values of the CWD are located at the northern part of the basin. CWD for the entire basin ranges between 10 and 250 mm. Furthermore, the trend of

the CDD varies between -18 to 10 days/decade. This is a slightly increasing trend compared to RCP 4.5. However, the most increasing trends are located at the northern part of the basin with values between 0 and 10 days/decade. There is a generally decreasing trend of CWD with values between -18 and 0 days/decade. Also, the trends in CDD and CWD are most significant at 95% confidence level throughout the basin (7 e and f).

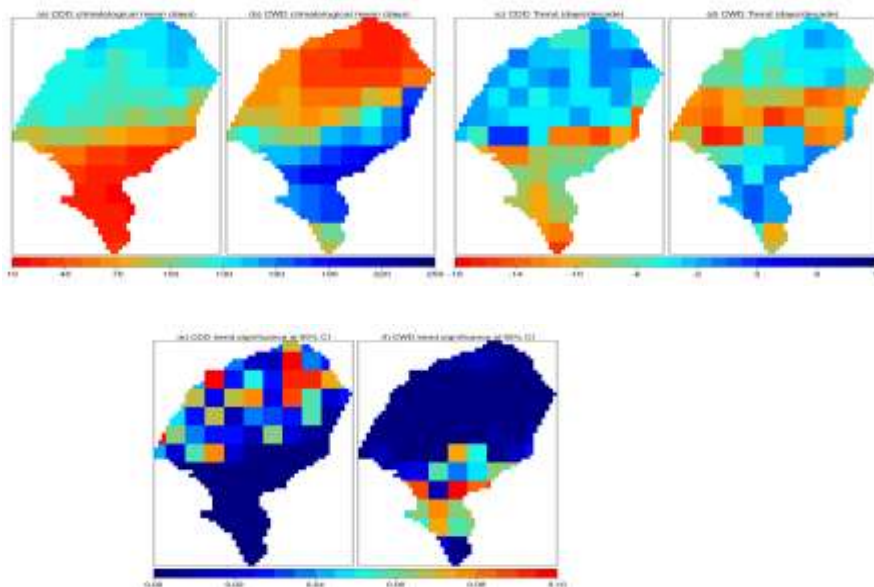


Figure 10: Climatological mean (a and b), trend (c and d) and trend significance (e and f) in CDD and CWD in the basin

Total annual rainfall from heavy rain days (R95p) and Total annual rainfall from very heavy rain days (R99p)

Figure 11 shows the climatological mean and trend of the total annual rainfall from

heavy rain days (R95p) and total annual rainfall from very heavy rain days (R99p) in the basin.

The climatological mean for the R95p ranges from 300 to 800 mm between 2030 and 2070 under RCP 8.5. This is an

increment of between 100 to 250 mm from the historical period. However, the lowest values are located in the northern part of the basin. The values for R99p range between 100 and 400 mm. Furthermore, there is a mixed trend of R95p in the basin. However, trend values of between -10 and 40 mm/decade are recorded in most parts of the basin. Similarly, the R99p trend

increases between 0 and 40 mm/decade in most parts of the basin. There is an increment in the magnitude of the trend compared to the future projection under RCP 4.5. Also, there is a mixed representation of significant and non-significant trends of R95p and R99p for the basin (11 e and f).

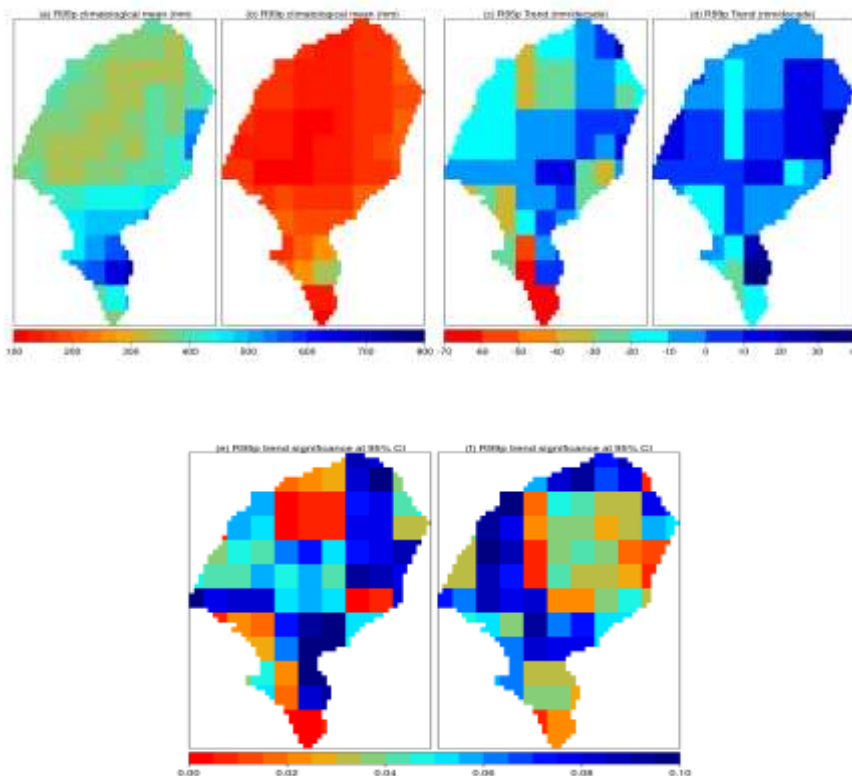


Figure 11: Climatological mean (a and b), trend (c and d) and trend significance (e and f) in R95p and R99p in the basin

Figure 12 shows the climatological mean and trend of the number of heavy rain days (r10mm) and total wet day rainfall (prcptot) in the basin.

Number of Heavy Rain Days (r10mm) and Total Wet Day Rainfall (prcptot)

The climatological mean for r10mm ranges from 25 to 80 mm between 2030 and 2050 under RCP 8.5. This is a decrease of 10mm in the upper bound from the projection period under RCP 4.5. The southern part of

the basin has the highest values of between 50 to 80 mm. Similarly, the lowest values of the prcptot are located in the northern part of the basin. The values of prcptot increase from 1000mm in the northern part to 2200mm in the southern part. Although the lower bound increases by 100 mm, the upper bound also decreases by 100 mm. Moreover, the trend of the r10mm decreases generally in the entire basin with

values between -1 and -7 mm/decade. There is a generally decreasing trend of prcptot in the basin with values between -100 and -20 mm/decade. Although, some patches of the southern part of the basin records increasing trends up to 20 mm/decade. Also, there is a predominant significant trend of r10mm and prcptot in the basin, (12 e and f).

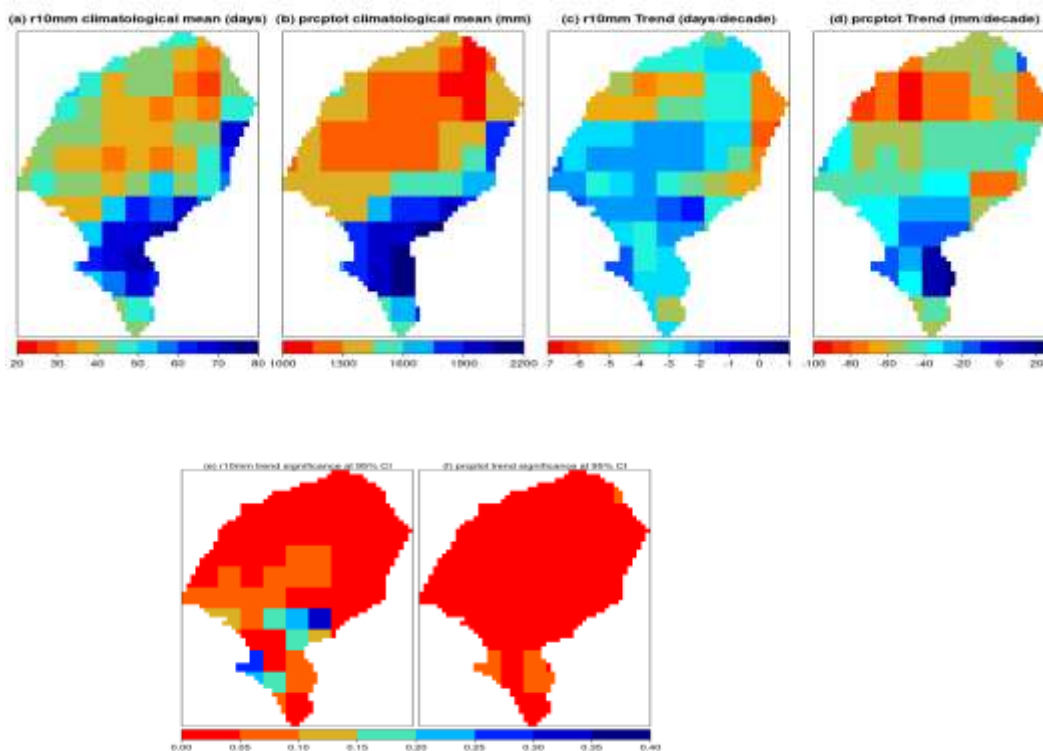


Figure 12: Climatological mean (a and b), trend (c and d) and trend significance (e and f) in r10mm and prcptot in the basin

Conclusion

Precipitation over the study area during the historical period shows a

decreasing trend in response to climate change. This does affect the changes in precipitation extremes over the region. The changes were observed to vary spatially during the historical baseline period. The combination of the increasing trend of the consecutive dry days index and decreasing trend of consecutive wet days signifies the ORB being susceptible to drought

occurrence during the historical period. The total annual rainfall from both heavy and very heavy days shows a higher trend increase in the Southern part of the basin and the Northern part of the basin shows a lower trend increase in the Northern region. This could potentially lead to increased runoff in the river basin and enhance the risk of flooding in the region especially the southern part of the region. The same spatial variation in the trend change is observed for the Number of heavy rain days and the total wet days during the historical baseline period.

Over the projection periods under both scenarios increasing trend of consecutive dry days, R99p and total annual rainfall signifies a more intense rainfall over reduced number of days. This thus makes the region susceptible to flash flood occurrence over the basin. Also, the decreasing trend observed for the r10mm and prcptot indices suggests that the basin is susceptible to increased frequency of drought occurrence over the projection period. While both scenarios agree to increased frequency of climate extremes over the basin, the RCP8.5 shows potential of more severe extreme conditions than the RCP4.5 scenario.

Acknowledgment

The authors would like to acknowledge and express their sincere gratitude to the Tertiary Education Trust Fund (TETFUND) for providing financial support for this research project. The funding provided by TETFUND has been instrumental in enabling the successful completion of this work. We would also like to thank the management and staff of TETFUND for their guidance and support throughout the project.

References

- Abiodun, B. J., Adegoke, J., Abatan, A. A., Ibe, C. A., Egbebiyi, T. S., Engelbrecht, F., & Pinto, I. (2017). Potential impacts of climate change on extreme precipitation over four African coastal cities. *Climatic Change*, 143, 399-413.
- Adeyeri, O. E., & Ishola, K. A. (2021). Variability and Trends of Actual Evapotranspiration over West Africa: The Role of Environmental Drivers. *Agricultural and Forest Meteorology*, 308, 108574.
- Adeyeri, O. E., Lawin, A. E., Laux, P., Ishola, K. A., & Ige, S. O. (2019). Analysis of climate extreme indices over the Komadugu-Yobe basin, Lake Chad region: Past and future occurrences. *Weather and climate extremes*, 23, 100194.
- Akinsanola, A. A., Ogunjobi, K. O., Ajayi, V. O., Adefisan, E. A., Omotosho, J. A., & Sanogo, S. (2017).

Comparison of five gridded precipitation products at climatological scales over West Africa. *Meteorology and Atmospheric Physics*, 129, 669-689.

Eltahir, B. A., & Gong, D. (2002). Regional climate impacts of increasing atmospheric CO₂ and land use change. *Journal of Hydrometeorology*, 3(6), 651-664.

Dosio, A., & Panitz, H. J. (2016). Climate change projections for CORDEX-Africa with COSMO-CLM regional climate model and differences with the driving global climate models. *Climate Dynamics*, 46, 1599-1625.

Longe, E. O., Omole, D. O., Adewumi, I. K., & Ogbiye, S. A. (2010). Water resources use, abuse and regulations in Nigeria. *Journal of Sustainable Development in Africa*, 12(2), 35-44.

Madden, R. A., & Williams, J. (1978). The correlation between temperature and precipitation in the United States and Europe. *Monthly Weather Review*, 106(1), 142-147.

Mao, Y., Nijssen, B., & Lettenmaier, D. P. (2015). Is climate change implicated in the 2013–2014 California drought? A hydrologic perspective. *Geophysical Research Letters*, 42(8), 2805-2813.

Mason, S. J., & Joubert, A. M. (1997). Simulated changes in extreme rainfall over southern Africa. *International Journal of Climatology: A Journal of the Royal Meteorological Society*, 17(3), 291-301.

Nicholls, N. (2004). The changing nature of Australian droughts. *Climatic change*, 63(3), 323-336.

Nicholson, Sharon E. "On the factors modulating the intensity of the tropical rainbelt over West Africa." *International Journal of Climatology: A Journal of the Royal Meteorological Society* 29.5 (2009): 673-689.

Okogbue, E.C., Balogun, I.A., Akinbobola, A., Adeyeri, O., Oluleye, A., Ajayi, V.O., Akinluyi, F.O., Akinwumiju, A.S., and Ige, S.O. (2021). GIS-based Analysis of Drainage Morphometry and Landuse/Landcover Dynamics in the River Ogun-Osun Basin, Southwestern Nigeria. *Journal of Sustainable Technology, Centre for Research and Development Federal University of Technology, Akure*, Vol. 11, No. 2 (November, 2021), ISSN: 2251-0680

Pinto, I., Lennard, C., Tadross, M., Hewitson, B., Dosio, A., Nikulin, G., ... & Shongwe, M. E. (2016).

Evaluation and projections of extreme precipitation over southern Africa from two CORDEX models. *Climatic Change*, 135, 655-668.

Reynolds, L. V., & Shafroth, P. B. (2017). Riparian plant composition along hydrologic gradients in a dryland river basin and implications for a warming climate. *Ecohydrology*, 10(6), e1864.

Rusticucci, M., & Penalba, O. (2000). Interdecadal changes in the precipitation seasonal cycle over Southern South America and their relationship with surface temperature. *Climate Research*, 16(1), 1-15.

Samuelsson, P., Jones, C. G., Will' En, U., Ullerstig, A., Gollvik, S., Hansson, U. L. F., ... & Wyser, K. (2011). The Rossby Centre Regional Climate model RCA3: model description and

performance. *Tellus A: Dynamic Meteorology and Oceanography*, 63(1), 4-23.

Seydou, T. H., Agali, A., Aissatou, S., Seydou, T. B., Issaka, L., & Ibrahim, B. M. (2023). Evaluation of the Impact of Seasonal Agroclimatic Information Used for Early Warning and Farmer Communities' Vulnerability Reduction in Southwestern Niger. *Climate*, 11(2), 31.

Shongwe, M. E., Van Oldenborgh, G. J., Van Den Hurk, B. J. J. M., De Boer, B., Coelho, C. A. S., & Van Aalst, M. K. (2009). Projected changes in mean and extreme precipitation in Africa under global warming. Part I: Southern Africa. *Journal of climate*, 22(13), 3819-3837.

Teutschbein, C., & Seibert, J. (2013). Is bias correction of regional climate model (RCM) simulations possible for non-stationary

conditions?. *Hydrology and Earth System Sciences*, 17(12), 5061-5077.

Trenberth, K. E., & Shea, D. J. (2005). Relationships between precipitation and surface temperature. *Geophysical Research Letters*, 32(14).

Trenberth, K. E., & Shea, D. J. (2005). Relationships between precipitation and surface temperature. *Geophysical Research Letters*, 32(14).

Vano, J. A., & Lettenmaier, D. P. (2014). A sensitivity-based approach to evaluating future changes in Colorado River discharge. *Climatic Change*, 122, 621-634.

Williams, A. P., Seager, R., Abatzoglou, J. T., Cook, B. I., Smerdon, J. E., & Cook, E. R. (2015). Contribution of anthropogenic warming to California drought during 2012–2014. *Geophysical Research Letters*, 42(16), 6819-6828.